13.1 Turbulence Considerations for Comparing Ecosystem Exchange over Old-Growth and Clear-Cut Stands with Limited Fetch and Complex Canopy Flows

Sonia Wharton*[1], Kyaw Tha Paw U[2], Matt Schroeder[3,4], Ken Bible[3,4] and Matthias Falk[2,5]

[1]Atmospheric, Earth and Energy Division, Lawrence Livermore National Laboratory, Livermore, CA
[2] Dept. Land, Air and Water Resources, University of California at Davis, Davis, CA
[3] Wind River Canopy Crane Research Facility, Gifford Pinchot Natl. Forest, Washington
[4]College of Forest Resources, University of Washington, Seattle, Washington
[5]CMCC, Euro-Mediterranean Centre for Climate Change, Lecce, Italy

1. ABSTRACT

Carbon dioxide, water vapor, and energy fluxes were measured using the eddy covariance (EC) technique over three adjacent evergreen conifer forests in southern Washington State to identify the effects of stand-age on ecosystem exchange. The sites represent Douglas-fir forest ecosystems at two contrasting successional stages: old-growth (OG) and early seral (ES). Here we present eddy flux and meteorological data from two ES stands and the Wind River AmeriFlux old-growth forest during the 2006 and 2007 growing seasons. We show an alternative approach to the usual friction velocity (u_*) method for determining periods of adequate atmospheric boundary layer mixing based on the ratio of mean horizontal (U) or vertical ($\overline{w}$) wind flow to a modified turbulence kinetic energy scale (u_{TKE}). The new turbulence parameters in addition to footprint modeling showed that daytime CO_2 fluxes (F_{NEE}) in small clear-cuts (< 10 hectares) can be measured accurately with EC if micrometeorological conditions are carefully evaluated. Overall, we measured lower evapotranspiration (OG = 230 mm; ES = 297 mm) and higher midday F_{NEE} (OG F_{NEE} = -9.0 µmol m^{-2} s^{-1}; ES F_{NEE} = -7.3 µmol m^{-2} s^{-1}) at the old-growth forest than at the ES sites during the summer (May-August). This study contributes critical land-atmosphere exchange data for two rarely studied Douglas-fir age classes.

2. INTRODUCTION

The Pacific Northwest region of the U.S. is one of the most productive forested areas in the world and its future role in the terrestrial carbon cycle will be dependent on how silviculture practices alter the age structure of these forests (Song and Woodcock 2002). Over the past 50 years, staggered-set clear-cutting on local Federal lands has created a fragmented landscape of different age Douglas-fir forests ranging from early seral (ES) (0–15 years), young (15–80 years), intermediate (80–200 years), mature (200–400 years), to old-growth (OG) (approximately greater than 400 years old). While early seral stands can compromise up to 40% of total forest coverage in the Western Cascade Mountains (Cohen et al. 1996) and are an essential component of the regional carbon budget, ecosystem exchange within this youngest age class has not been thoroughly studied with eddy covariance (EC).

Often early seral stands are the result of a size-restricted harvest on Federal lands and thus have very limited fetch. This creates a unique set of micrometeorological concerns for the eddy covariance technique. A desirable fetch-to-instrument height ratio is dependent on atmospheric boundary layer (ABL) stability and surface-canopy roughness but has generally been accepted at ~ 40:1 (e.g., Kruijt 1994, Schmid 1994, Irvine et al. 1997). Fetch requirements in small, individual forest stands (e.g., clear-cuts) within a heterogeneous vegetative area are less certain and may be more site-specific. Fetch is further complicated by variable topography which creates complex wind flows including strong, along-valley-axis flows (wind direction shifts) and gravity-driven, mountain-valley flows that are particularly strong at night.

Ecosystem responses to seasonal climate (e.g., summer drought), the timing of extreme weather events (e.g., summer rain pulses), and phenological changes (e.g., bud break) likely vary with stand age and affect biosphere-atmosphere exchange, and yet our understanding of these stand-level, age-effects remains limited for Douglas-fir forests. The goals of this study are to: (1) determine whether mass and energy fluxes can be accurately measured in typical Douglas-fir early seral stands of the Pacific Northwest and (2) identify any stand-age differences in CO_2 and H_2O fluxes between the old-growth and early seral stands.

3. METHODS AND MATERIALS

3.1 Site Description

Despite the surrounding complex terrain of the Western Cascade Mountains, all three forest stands are located in a relatively flat valley in southern Washington State. The predominant wind direction is from the west although valley flow (northwest-southeast) wind shifts are also common. The climate is dominated by two distinct seasons: a cool, wet winter and a warm, dry summer. Very little rain (<10% of 2233 mm annual average) typically falls from July through August and consistent precipitation usually does not return to the area until the end of October. Mean annual temperature is 8.7 ^{o}C; mean minimum temperature is 2.5 ^{o}C.

* *Corresponding author address*: Sonia Wharton, Atmospheric, Earth and Energy Division, L-103, PO Box 808, Lawrence Livermore National Laboratory, Livermore, CA 94551. Email: wharton4@llnl.gov
Web: http://atm.ucdavis.edu/~swharton/research.html

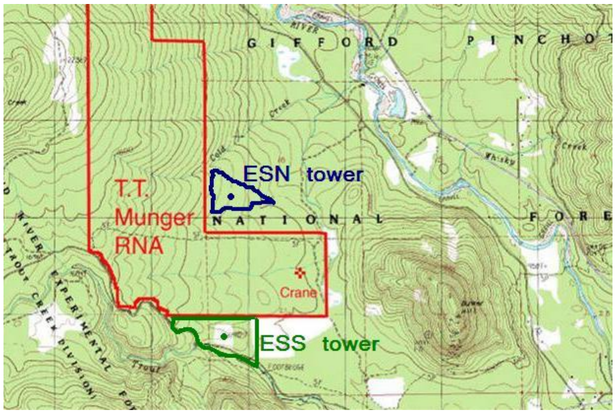

Figure 1. Site locations of the old-growth (red), Early Seral North (blue) and Early Seral South (green) stands.

Brief site characteristics are listed here while more detailed descriptions are found in Shaw et al. (2004) and Harmon et al. (2004) for the old-growth forest and Wharton et al. (2009a) and Wharton et al. (2009b) for the early seral stands. The Wind River Canopy Crane (45.821 N, -121.952 W) is located in the T.T. Munger Research Natural Area (Figure 1), an old-growth (OG) forest ecosystem that is composed primarily of late seral stage Douglas-fir (*Pseudotsuga menziesii*) and western hemlock (*Tsuga heterophylla*). The forest represents the near endpoint of several gradients: age (400-500 years), biomass (619 Mg C ha^{-1}), structural vertical complexity, and tree height (max = 65 m) (Harmon et al. 2004, Parker et al. 2004, Shaw et al. 2004). The Early Seral North (ESN) flux tower (45.827 N, -121.960 W) was located in a recent (1994) clear-cut (7 ha), 1.25 km northwest of the canopy crane (Fig 1). In 1997 the clear-cut was seeded with Douglas-fir saplings at a density of 741 trees/ha. The Early Seral South (ESS) flux tower (45.813 N, -121.959 W) was located in an abandoned clear-cut (1990), 1.1 km southwest of the canopy crane (Fig 1), and was naturally established with Douglas-fir (the pioneering species) from surrounding cone crops. Additional stand details are listed in Table 1.

	Early Seral North	Early Seral South	Old-Growth Stand
Stand properties			
maximum tree age (years)	10	14	~ 450–500
stand area (ha.)	7	10	478
slope (%)	< 10	< 5	3.5
disturbance	1st harvest in 1920, 2nd harvest in 1994	1st harvest in 1920, 2nd harvest in 1990	catastrophic fire ~1500
site preparation	minimal: coarse woody debris (CWD) left on site	extensive: all CWD removed from site, soil tilled	none: natural fire recovery, very high CWD
mean h_c (m)	4.4	3.6	50–60
EC height (m)	5.5	5	67
LAI (m^2 m^{-2})	1.1–1.8	0.6–1.1	8.2–9.2
foliar N %; foliar C:N	1.2; 44:1 ± 3	1.4; 37:1 ± 3	1.2; 41:1
root depth (m)	most within 0.3, max 0.5	most within 0.3, max 0.5	most within 0.5, max1-2 m
Soil properties			
sand:silt:clay	66:28:6	62:29:9	60:31:9
organic C (%); C:N	2.9; 27:1 ± 6	3.9; 26:1 ± 3	5-10; 25:1 ± 1
bulk density (g cm^{-3})	0.94	1.07	0.83

Table 1. Site disturbance history, canopy, and soil characteristics for the three stands.

3.2 Instrument Details

EC and micrometeorological data were measured continuously at the old-growth forest from January–December 2006 (OG06) and January–December 2007 (OG07) although winter data are not presented here. Data were collected at Early Seral North (ESN06) during the 2006 growing season and at Early Seral South (ESS07) during the 2007 growing season. Growing season is defined here as March through October; drought season as July through October.

Old-growth forest

The eddy-covariance (EC) system consisted of a closed path Infrared Gas Analyzer (LI-COR 7000, LI-COR Inc., Lincoln, Nebraska, USA) and an ultrasonic anemometer (Solent HS, Gill Instruments, Lymington, England, UK), both mounted at 67 m on an 85 m tall canopy crane. The EC system measured CO_2 and H_2O vapor mixing ratios and wind velocities at 10 Hz. Soil moisture was measured with four soil moisture probes at incremental depths from 20 to 200 cm (Sentek EnviroSMART, Sentek Sensor Technologies, Stepney, Australia). Soil temperature (107B, Campbell Scientific, Logan, Utah, USA) was measured in replicate at depths of 0, 15, 30 cm. Additional instrumentation included a 4-stream net radiometer (CNR-1, Kipp & Zonen, Delft, The Netherlands) at 85 m, up- and down-facing PAR sensors (190SB, LI-COR) at 67 m, HFT-3.1 (REBS, Seattle, Washington, USA) soil heat flux plate buried 7.5 cm below the surface, air temperature/humidity sensor (HMP-35C, Vaisala Oyj, Helsinki, Finland) at 67 m and barometric pressure sensor (CS105, Vaisala) at 67 m.

The anemometer faced west towards the maximum area of homogenous vegetation (1-2 km). Footprint modeling (following analytical solutions given by Wilson and Swaters 1991) was done by Paw U et al. (2004) and Falk (2005). Their results showed that the source area affecting the vertical flux at the canopy crane is within the old-growth forest for most wind directions under unstable conditions but extends outside the stand during very stable conditions.

Early Seral stands

Eddy-covariance estimates of vertical H_2O and CO_2 fluxes were made at both early seral stands using a CSAT-3 sonic anemometer (Campbell Scientific) and an open-path fast response Infrared Gas Analyzer (LI-COR 7500) which measured the velocity vectors, sonic temperature, and densities of CO_2 and H_2O vapor at 10

Hz. Micrometeorological measurements of above canopy air temperature/relative humidity (HMP-35C, Vaisala), net radiation (Q7, REBS), incoming and outgoing PAR (190SB, LI-COR), soil temperature (5, 10 and 15 cm) (CS106B, Campbell Scientific), soil water content (0-30, 30-60, 60-90 cm) (TDR100, Campbell Scientific), and ground heat flux (7.5 cm) (HFT-3.1, REBS) were also measured.

At ESN, the sonic anemometer was mounted facing west-southwest, pointing in the direction of greatest homogeneous fetch (200 m from the western stand edge). Both the LI-7500 and CSAT-3 were mounted at 5.5 m a.g.l., 1.5 m above the ESN canopy, on a boom extending from a 6m tall tower.

At ESS, the sonic anemometer was mounted in the southerly direction to reduce the frequency of tower-shadowing: diurnal valley flow produced winds that occurred 50% of the time from the west and 50% of the time from the east. Both the LI-7500 and CSAT-3 were mounted at 5.0 m a.g.l, 1.5 m above the ESS canopy.

3.3 Flux Calculations and Corrections

Old-growth forest

Carbon dioxide (F_c) (µmol CO_2 m^{-2} s^{-1}), water vapor (F_{H2O}) (mmol H_2O m^{-2} s^{-1}), latent energy (λE) (W m^{-2}) and sensible heat (H) (W m^{-2}) fluxes were computed with FORTRAN90 code using a 30-minute averaging time and a horizontal coordinate rotation. The rate of change in CO_2 concentration (storage flux, S_c, µmol CO_2 m^{-2} s^{-1}) within the canopy volume was estimated on a half-hourly basis using time changes in the mean CO_2 mixing ratio measured at the top of the canopy. To account for CO_2 stored within the canopy and below the detection height of the instruments, S_c was added to F_c to estimate net ecosystem exchange of carbon (F_{NEE}, µmol CO_2 m^{-2} s^{-1}) on a half-hourly basis. F_{NEE} and λE were further screened for incomplete half-hours, general instrument failure (e.g., pressure problems in the closed-path EC system), non-preferred wind directions (45° to 180°), major rain or snow events, or significant outliers (above or below the 95th confidence intervals) and gap-filled for missing values (using a running-mean approach, Reichstein et al. 2005). For further details on post-processing at the old-growth stand see Paw U et al. (2004), Falk (2005) and Falk et al. (2008).

Early seral flux towers

At the two early seral stands F_c, F_{H2O}, λE, and H were calculated in real-time from 10 Hz data using the CR1000 eddy covariance program (Campbell Scientific). The flux program used a 30-minute averaging period and included WPL80 (Webb et al. 1980) density corrections to eliminate air density fluctuation effects on CO_2 and H_2O fluxes. During post-processing all mass and energy fluxes were re-calculated after the mean cross-wind and mean vertical wind velocities were forced to zero. The rate of change of CO_2 concentration (S_c) within the canopy was estimated using the half-hourly changes in the CO_2 mixing ratio measured at the top of the canopy and was added to F_c to estimate F_{NEE}.

Data screening criteria at ESN and ESS

The early seral flux data necessitated a different screening protocol than the old-growth data for various reasons. Full details can be found in Wharton et al. (2009a). Most importantly the fetch availability and turbulence-induced edge effects (from an abrupt rough-to-smooth canopy roughness transition) were a much higher concern at the early seral stands and warranted the creation of data criteria 5 and 6 as described below.

Half-hour F_{NEE}, F_{H2O}, and energy fluxes were excluded from the time series if one or more of the following criteria were met: (1) instrument malfunction or incomplete half-hour, (2) “tower shadowing” or flow distortion around the CSAT-3, (3) heavy precipitation, (4) spike filter = 1 (F_c only), (5) ratio of mean vertical or horizontal wind flow to turbulent velocity scale was greater than the critical threshold, (6) insufficient fetch, or (7) half-hourly variance was greater than the 95th and less than the 5th confidence intervals. We used a spike filter methodology in criterion 4 to detect significant half hour CO_2 anomalies or outliers in the time series as described in Papale et al. (2006). The spike filter methodology removed 5% of available F_c data at ESN and 7% at ESS.

Criterion 5 was used to identify half hour fluxes measured during conditions when transport by mean flow could no longer be neglected compared to turbulent flow in the wind field. This concern is shown by studying the Reynolds-averaged mass balance equation for biosphere-atmosphere exchange of CO_2:

$$\frac{\partial \overline{\rho_c}}{\partial t} + \frac{\partial (\overline{u_i}\,\overline{\rho_c})}{\partial x_i} + \frac{\partial (\overline{u'_i\,\rho'_c})}{\partial x_i} = \overline{S_c} \qquad (1)$$

Eq (1) shows that the CO_2 source or sink magnitude (net ecosystem exchange when integrated over the height of the canopy), $\overline{S}_c$, equals the sum of three terms: the rate of change in CO_2 storage (first term on LHS, estimated from measurements), the collective horizontal and vertical advection terms (second term, not measured or directly estimated here) and the collective eddy covariance terms (third term, the measured vertical flux and flux divergences not measured or directly estimated here). The contribution of CO_2 exchange from the flux divergence terms is considered here to be negligible.

To assess the contribution of turbulent transport to net ecosystem exchange, we first assumed that the efficiency of turbulence to transport mass and energy could be represented by the magnitude of turbulence kinetic energy (TKE). We then defined two turbulence intensity parameters I_w and I_U based on the ratio of mean vertical ($\overline{w}$, m s^{-1}) or horizontal (U, m s^{-1}) wind velocity to a modified turbulence velocity scale (u_{TKE}, m s^{-1}), where u_{TKE} is defined as,

$$u_{TKE} = \sqrt{(\overline{u'^2} + \overline{v'^2} + \overline{w'^2})} \qquad (2)$$

and $\overline{u'^2}$, $\overline{v'^2}$ and $\overline{w'^2}$ are mean variance in the stream-wise, cross-wise and vertical velocity directions, respectively.

Note that u_{TKE} now has the same dimensions as the original velocity variables (m s^{-1}). We calculated a vertical turbulence intensity ratio, Eq (3),

$$I_w = \frac{\overline{w}}{u_{TKE}} \tag{3}$$

to determine conditions when transport by mean vertical wind flow (measured $\overline{w}$) could no longer be neglected compared to turbulent eddy flow. This value is called the critical I_w threshold (I_{wcrit}). Since vertical velocity is hard to measure with high accuracy and is subject to errors associated with miss-leveling of the sonic anemometer, we made site-specific I_w thresholds and assumed that no significant changes in the precision of $\overline{w}$ measurements occurred during the study period for any given anemometer. A horizontal turbulence intensity ratio was likewise calculated using Eq (4),

$$I_U = \frac{U}{u_{TKE}} \tag{4}$$

to determine the contributions of transport by mean horizontal wind flow to turbulent eddy flow. If $I_U > I_{Ucrit}$ or $I_w > I_{wcrit}$, advective transport of energy, mass and momentum was considered non-negligible compared to the turbulent transport and the eddy fluxes were gap-filled. Note that I_U and I_W are the reciprocal of the more traditional definition of turbulence intensity (e.g., Stull 1988).

We chose to use a modified turbulence velocity scale (u_{TKE}) instead of the commonly used surface friction velocity (u_*) to infer ABL mixing conditions. Friction velocity is routinely used in EC studies as a filter for identifying (and removing) CO_2 flux measurements taken during inadequate nighttime turbulence (called the "u-star correction method," Goulden et al. 1996; see also e.g., Aubinet et al. 2000; Massman and Lee 2002) We contend that using u_* is not the most ideal way of determining turbulence in clear-cut stands because (1) limited fetch requires that daytime mixing conditions also be screened and u_* includes only mechanically-produced turbulence, and is thus not a good indicator of the total amount of turbulence present during daylight hours, (2) intermittent, buoyancy-driven turbulence can occur at night over landscapes with canopy roughness changes and complex terrain, and non-shear turbulence will not be captured by the u_* parameter, (3) under certain ABL conditions (e.g., mesoscale exchange) turbulent fluxes are small but u_* indicates highly turbulent conditions, and vice versa, there are times when turbulent fluxes are nonzero but u_* suggests no turbulence (Acevedo et al., 2009), and (4) under certain ABL conditions (e.g., unstable with low wind speeds) the momentum sink is absent and u_* is zero but scalar sources are present and the turbulent exchange is nonzero.

Based on the principles used in eddy covariance theory, u_* is not an independent state variable when used to filter CO_2 fluxes. Eq (5) shows that u_* is defined from the stream-wise and cross-wise momentum fluxes,

$$u_*^2 = \sqrt{(\overline{u'w'}^2 + \overline{v'w'}^2)} = \frac{|\tau_{Reynolds}|}{\overline{\rho}} \tag{5}$$

where the Reynolds stress ($\tau_{Reynolds}$) is calculated from the vector-sum of the individual surface stresses, τ_{uw} and τ_{vw}, Eqn (6),

$$|\tau_{Reynolds}| = \sqrt{(\tau_{uw}^2 + \tau_{vw}^2)} \tag{6}$$

Therefore, friction velocity is really a flux and is the result of the momentum sink, while u_{TKE} is instead conceptually linked to the independent ability of turbulence to transfer mass and energy through the ABL. The u_{TKE}-derived variables in Eqns. 2-4 are all direct measures of turbulence.

3.4 Footprint Modeling

A simple, parameterized footprint model (Kljun et al. 2004; http://footprint.kljun.net/index.php) was used in criterion 6 to determine the extent of which measured turbulent fluxes were influenced by scalar sources outside of the early seral stands. A footprint size and shape varies according to receptor height (here the EC measurement height), surface or canopy roughness, and planetary boundary layer mixing conditions during which the fluxes were measured (i.e., the ratio of advective to turbulent transport). While the chosen model relies on a simplified scaling approach for the footprint functions, it has been thoroughly tested with a more complex 3-D Lagrangian stochastic footprint model (Kljun et al. 2002). The estimated footprint (x_R) is calculated using user-defined values of standard deviation of vertical wind velocity (σ_w), friction velocity (u_*), planetary boundary layer height (we used 1500 m during daytime and 600 m at nighttime), zero displacement height ($z_o = 0.10h_c$, where h_c is the canopy height) and EC measurement height. In this study all footprint estimates were based on x_R, the distance from the flux tower which includes 80% of the source area influencing the EC flux measurement. For the model runs, we separated all turbulence data first into daytime (10:00–14:00) and nighttime (24:00–2:00) classes, and secondly into wind direction sectors (eight 45º bins).

4. RESULTS

4.1 Climatic Conditions

The annual mean air temperature was near the long-term (1977–1997) average (8.8 °C) in both 2006 (8.9 °C) and 2007 (8.7 °C). Total water-year (October through September) precipitation was also near average (2366 mm) in 2006 (2361 mm) and 2007 (2129 mm). Although 2006 and 2007 were similar in terms of total precipitation and mean annual temperature, the spring and summer seasons were in fact climatologically distinct. Spring 2006 was cooler and wetter (409 mm) and led into a very dry (72 mm) and warm (17.2 °C) drought season. In 2007, the spring months were drier (217 mm) than in 2006 although late-season rains made the summer much wetter (316 mm) and cooler (16.4 °C). For comparison, the long-term averages for the drought season are 314 mm and 16.2 °C.

The early seral stands were warmer and less humid than the dense old-growth forest during summer daylight hours. Average May–August VPD was 1.6 kPa at ESN06 and 1.2 kPa at OG06, and 1.3 kPa at ESS07 and 1.1 kPa at OG07 during the hours of 10:00–16:00. Soil moisture also varied amongst stands and years although the drought-season pattern remained a dominant feature. Near-surface (0-30 cm depth) θ_v was similar at both ESN06 and OG06: after June soil moisture began to steadily decrease and approached 0.15 $m^3\ m^{-3}$ until rains returned to the area in October. At ESS07, 0–30 cm θ_v did not drop below 0.20 $m^3\ m^{-3}$ while the near-surface θ_v approached 0.15 $m^3\ m^{-3}$ at OG07. Deeper measurement depths revealed that while near-surface θ_v at OG07 fell below the critical threshold of 0.2 $m^3\ m^{-3}$ for inducing ecosystem water stress (Falk et al. 2005, 2008), θ_v in the rooting zone (1 to 1.5 meters) stayed above 0.3 $m^3\ m^{-3}$. Daily maximum soil temperatures were higher at the early seral stands and differences up to 15 °C were observed between ESS07 and OG07.

4.2 Turbulence Statistics and Footprint Modeling

Half-hour measurements of u_* and I_U at ESN and ESS are shown in Figure 2. Maximum friction velocity and I_U did not occur together, instead maximum u_* values were observed when I_U showed intermediate values between 0.5 and 1.0. As I_U approached zero (mean wind velocity << vertical turbulence velocity), u_* actually indicated less turbulent conditions. There were also a large number of half hours when u_* was near zero and suggested very low turbulence conditions while I_U showed a high degree of turbulence (0.0 and 0.5).

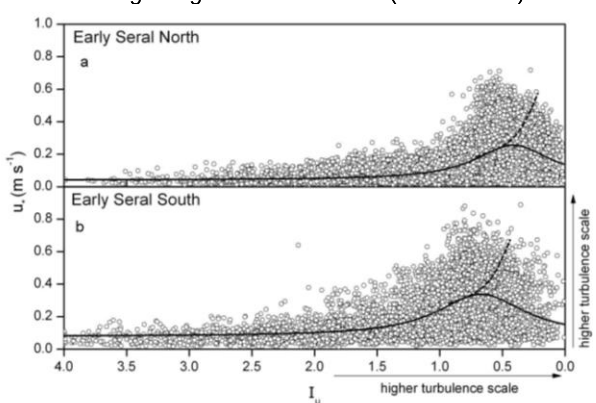

Figure 2. Half-hourly magnitudes of u_* and I_U at ESN and ESS. The line of best fit is described with a Lorentz peak function (solid black line). Note that u_* decreases at the highest I_U ratios (i.e., times when advection can be neglected and U_{TKE} is high) instead of following an expected exponential decay function (dashed line).

The critical thresholds for insufficient turbulent mixing were determined to be: I_{Ucrit} = 1.5 at ESN and I_{Ucrit} = 2.0 at ESS, and I_w = |0.15| at ESN and I_w = |0.15| at ESS. We determined these thresholds based on the time series mean plus one standard deviation. We checked their accuracy by also examining:

(1) Footprint modeling. We found that when $I_U > I_{Ucrit}$ or $I_w > I_{wcrit}$, the flux footprints extended beyond the clear-cut stands over 90% of the time.

(2) Flux statistics. During conditions when $I_U > I_{Ucrit}$ we observed a "leveling-off" or systematic decline to zero in the daylight fluxes. For example, when $I_U > I_{Ucrit}$, mean F_{NEE} was 0.77 µmol $m^{-2}\ s^{-1}$ at ESN (2006) and -0.36 µmol $m^{-2}\ s^{-1}$ at ESS (2007), compared to -6.3 µmol $m^{-2}\ s^{-1}$ (ESN06) and -4.3 µmol $m^{-2}\ s^{-1}$ (ESS07) when $I_U < I_{Ucrit}$. We also looked at how sensitive the sensible heat flux was to our choosing of a critical turbulence threshold based on u_{TKE} instead of u_*. Figure 3 shows that a greater number of "real" daytime H fluxes would be excluded from the measurement period if a critical turbulence threshold was based on u_* rather than u_{TKE} at ESS07. 13% of sensible heat fluxes (mean = 53 W m^{-2}) were excluded using the u_{TKE} critical threshold while 21% (mean H = 86 W m^{-2}) were excluded using the u_* critical threshold. H fluxes > 150 Wm^{-2} during very low u_* conditions (checkered box) are probably "real" sensible heat fluxes since net radiation during these times was greater than 400 W m^{-2} nearly 90% of the time and the mean half-hour was noon (Fig 3a).

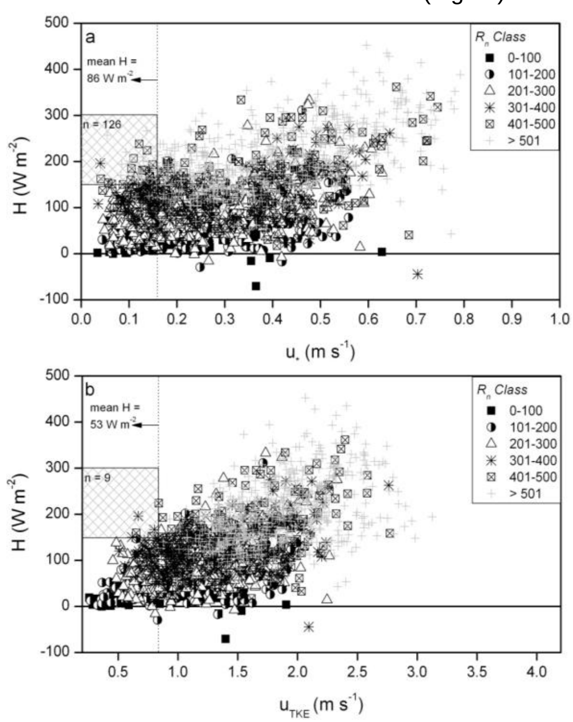

Figure 3. Daytime (10:00–16:00) sensible heat fluxes at ESS07 binned by net radiation under varying turbulence conditions shown by u_* (4a) or u_{TKE} (4b). The dashed line indicates a critical threshold for each turbulence parameter. The checkered boxes highlight H fluxes > 150 W m^{-2} which are most likely "real" but which would be excluded using u_{*crit} or $u_{TKEcrit}$.

Conditions when the mean flow contribution (i.e., possible advection from Bunker Hill to the east and Trout Creek Hill to the west) could no longer be a neglected component of the vertical flux are shown in Figure 4 for ESN. Non-negligible horizontal mean flow was more prevalent at ESN (2006) during nighttime hours than non-negligible vertical mean flow (frequency of 24 to1), while non-negligible vertical mean flow and horizontal mean flow conditions occurred in roughly equal frequencies at ESS (2007) (not shown). Also, non-negligible horizontal mean flow (I_U > 1.5) was occasionally observed (7.8%) at ESN during daylight hours (Fig. 3a) but not at ESS as very few daylight hours (< 1 %) approached I_{Ucrit}. Nighttime (2:00–4:00) flux footprints (x_R) extended at least 350 m in the westerly direction and went beyond the boundaries of both stands during high I_w and I_U conditions. Nighttime

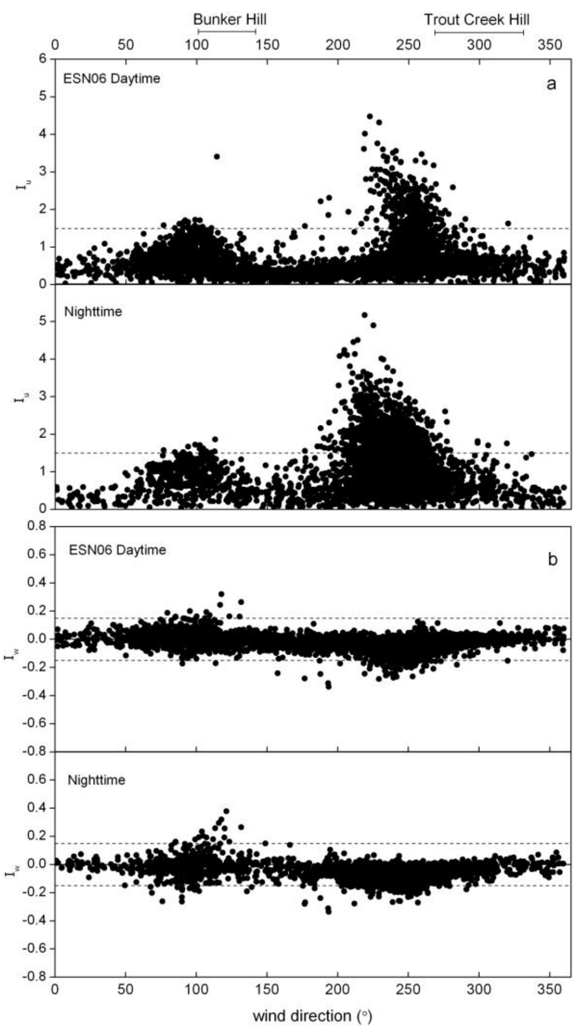

Figure 4. Half-hour (a) mean horizontal flow-to-turbulence intensity ratios and (b) mean vertical flow-to-turbulence intensity ratios for daytime and nighttime periods at ESN by wind direction. Critical values for I_U and I_W are indicated by the dashed lines. The directions of Bunker Hill and Trout Creek Hill are labeled.

fluxes measured while I_w and I_U were less than I_{wcrit} and I_{Ucrit} came from scalar sources closer to the towers (at least 200 m) but the flux footprints were still beyond the boundaries of the stands for most wind directions (82% and 85% of the time at ESN and ESS, respectively). For this reason, and because I_w and I_U went beyond the critical thresholds an additional 5% of the time at ESN and 13% at ESS, we do not include estimates of nighttime ecosystem exchange in this paper.

Midday (10:00–14:00) footprints (x_R) ranged from 75 m (east upwind direction) to 100 m (north upwind direction) at ESN and 77 m (east upwind direction) to 115 m (north upwind direction) at ESS, and require fetch-to-instrument ratios ranging from 14 to 23:1. Available fetch:instrument ratios averaged 33:1 and 34:1 at ESN and ESS, respectively, but ranged from 10 to 44:1 depending on wind direction (Table 2). Most wind directions at ESN included footprints within the clear-cut stand. Greatest uncertainty arose when winds were from the southeasterly direction (23% of the data points) because these source footprints extended outside of the clear-cut stand into an adjacent 80-year old Douglas-fir forest. These fluxes were removed from the time series and gap-filled. At ESS, daytime footprints were less of a concern as nearly all upwind directions had sufficient fetch. The only exception was when winds arose from the northerly and southerly directions but this occurred less than 15% of the time.

4.3 Seasonal and Monthly Flux Dynamics

CO_2 uptake at the old-growth stand was highest in the spring before bud break when air and soil temperatures and vapor pressure deficit were relatively low, and soil moisture and light levels were favorable for photosynthesis. Midday (10:00–14:00) CO_2 fluxes peaked seasonally in April at the old-growth stand and were -14.0 ± 3.4 μmol m^{-2} s^{-1} in 2006 (Fig. 5a) and -12.3 ± 2.1 μmol m^{-2} s^{-1} in 2007 (Fig. 5b). In contrast, April midday F_{NEE} magnitudes were significantly (P<0.0001) smaller (less net carbon uptake) at the early seral stands: - 4.0 ± 1.4 μmol m^{-2} s^{-1} at ESN06 and - 3.8 ± 1.3 μmol m^{-2} s^{-1} at ESS07. Maximum midday CO_2 fluxes were observed two to three months later in June and July at the early seral stands and coincided with peak LAI in the young canopies. Maximum CO_2 fluxes were measured in July at ESN06 (-10.2 ± 2.0 μmol m^{-2} s^{-1}) and in June at ESS07 (-8.7 ± 0.9 μmol m^{-2} s^{-1}), while net CO_2 uptake dropped sharply in June at the old-growth forest and continued to decline through the summer months in both 2006 and 2007.

E_T was relatively constant between April and June at the OG stand and a seasonal-summer decline was not observed until July in 2006 and August in 2007 (Fig. 5c,d). Strongest E_T seasonality was observed at ESN. June–August E_T averaged 85 mm per month while April–May E_T was 40 mm lower. Not enough data were available at ESS to make the same seasonal comparisons. Total May through August E_T was 305 ± 11 mm at ESN06 and 231± 9 mm at OG06, and 289 ± 9 mm at ESS07 and 230 ± 8 mm at OG07.

site	upwind direction	frequency	source footprint (x_R) (m)	available fetch (x_A) (m)	x_R: EC height	x_A: EC height	sufficient fetch? ($x_A > x_R$)
ESN	0–45	2%	83.5	80	15:1	14:1	no
	45–90	6%	75.8	150	14:1	27:1	yes
	90–135	23%	78.8	80	14:1	14:1	no
	135–180	12%	78.0	130	14:1	24:1	yes
	180–225	15%	83.4	170	15:1	30:1	yes
	225–270	28%	95.8	210	17:1	38:1	yes
	270–315	11%	99.3	240	18:1	44:1	yes
	315–360	3%	92.5	90	17:1	16:1	no
		72%			**16:1**	**33:1**	**yes**
ESS	0–45	4%	89.1	80	18:1	16:1	no
	45–90	29%	77.2	190	15:1	38:1	yes
	90–135	14%	83.0	200	17:1	40:1	yes
	135–180	5%	94.5	70	19:1	14:1	no
	180–225	13%	105.9	140	21:1	28:1	yes
	225–270	17%	105.3	160	21:1	32:1	yes
	270–315	14%	102.4	170	21:1	34:1	yes
	315–360	3%	114.2	50	23:1	10:1	no
		87%			**19:1**	**34:1**	**yes**

Table 2. Midday (10:00-14:00) footprint (x_R) and available fetch (x_A) distances for all wind directions at the early seral flux towers. The bolded text shows the percentage of time when the required fetch was available and for those times, mean source footprint to eddy covariance height ratio and mean available fetch to eddy covariance height ratio.

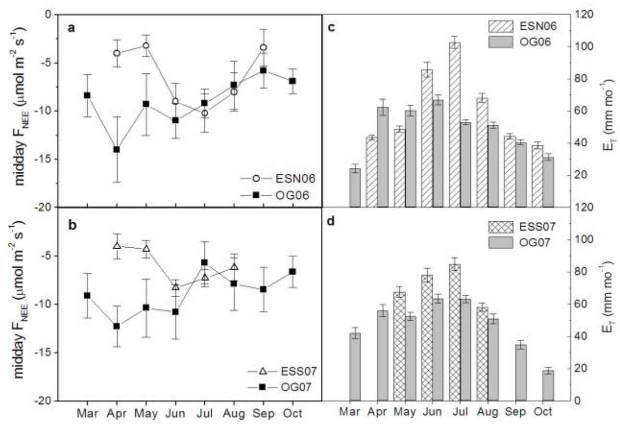

Figure 5. Mean midday CO_2 fluxes by month at (a) Early Seral North and the old-growth forest (2006) and (b) Early Seral South and old-growth (2007) show strong seasonal differences between the old and young stands. Total monthly evapotranspiration at (c) ESN06 and OG06 and (d) ESS07 and OG07. Error bars are bootstrapping uncertainties in the monthly fluxes.

5. DISCUSSION

5.1 Turbulence Parameters, I_w and I_U

Before we could confidently compare fluxes amongst stands we first needed to answer the question: Were the clear-cut patches large enough in size so that we were measuring fluxes over the vegetation of interest? We were not satisfied that the friction velocity scale was able indicate periods of inadequate turbulent mixing during both daytime and nighttime hours at the early seral stands so we created new parameters I_w and I_U. Our turbulence-intensity methodology for the early seral stands revealed that most of the nighttime CO_2 fluxes were measured during non-negligible vertical mean flow, non-negligible horizontal mean flow or from scalar sources outside the boundaries of the clear-cuts. These findings support the theoretical calculations made by Park and Paw U (2004) whose model predicted significant advection along abrupt forest edges. We decided not to include any nighttime CO_2 flux data in this paper because we feel that the EC technique was not accurately measuring turbulent CO_2 exchange at night (i.e., the respiration flux). For consistency we also did not include any nighttime data at the old-growth site. Other clear-cut studies have reported nighttime flux data for fetch limited stands including Kolari et al. (2004) and Humphreys et al. (2005). We suggest two primary reasons for why we in contrast rejected our nighttime flux data:

(1) *Differences in footprint and fetch*: Wind River ES tree height and fast growth rates required that we measure at least 5 m above the ground surface and in doing so we increased the footprint size so that it often extended beyond the stand boundaries. Humphreys et al. (2005) in comparison measured over a younger, shorter, and smoother Douglas-fir canopy which shifted the turbulence frequency distribution towards smaller eddies which requires smaller footprints to resolve. Our early seral stands also had a drastic rough-to-smooth surface change (the transition from a 40 meter, 80 year old forest to 4 meter, 10 year old forest) which also increased the amount of fetch needed to ensure that we were measuring within the atmospheric equilibrium layer. Our fetch:instrument height ratios from the footprint model were close to 35:1. This is slightly less than the general 40:1 rule given by Schmid (1994) but close to ratios given by van Breugel et al. (1999) and Kolari et al. (2004) for similar sized clear-cuts.

(2) *Differences in turbulence methodology*: Our paper introduces a novel method to determine adequate turbulence conditions for flux measurements. We suggest that a velocity scale based on TKE (e.g., u_{TKE}) is a more accurate way to assess ABL mixing because it

includes turbulence generated by buoyancy (nighttime gravity waves) as well as from mechanical forces. Also, turbulence regimes based on a u_* scale can be misclassified during mesoscale exchange while a TKE-based scale does not suffer from the same time-dependent variance errors (Acevedo et al. 2009). When the mass budget exchange equations, such as those presented by Lee (1998), Paw U et al. (2000), and Park and Paw U (2004) are carefully examined, it is clear that the kinematics of turbulent transport are related to the velocity fluctuations (in this case, as measured by u_{TKE}) and the kinematics of advective transport are driven by the mean velocity field.

The daytime EC data in our study were carefully screened by examining the footprint model, mean velocity-to-turbulence flow ratios, and energy budget closure, and we feel confident in reporting a high fraction of daytime ecosystem fluxes from the early seral stands. 28% and 13% of the daytime data at ESN and ESS, respectively, occurred when the footprint model runs indicated inadequate fetch and these data points were removed. I_U and I_w went beyond the critical thresholds occasionally during daylight hours and our observations correspond with studies by Feigenwinter et al. (2004) and Marcolla et al. (2005) which show that midday advective fluxes can make up to 10% of the eddy flux.

5.2 Stand-Age Effects on Ecosystem Fluxes

Bud break in Pacific Northwest Douglas-fir trees occurs in late spring to early summer and the production of new needles as well as the summer-time growth of ground species has significant impacts on a forest with very low biomass (LAI ~ 1 to 2 m^2 m^{-2}). We saw this in the early seral stands as peak CO_2 net uptake rates occurred in mid-summer. In contrast, phenological changes at the old-growth stand (LAI ~ 8 m^2 m^{-2}) did not significantly increase net carbon uptake as we observed maximum uptake rates in April. The occurrence of peak CO_2 fluxes during spring-time has also been observed at a Oregon old-growth Ponderosa pine forest (Law et al. 2000) and Vancouver Island intermediate-age Douglas-fir forest (Humphreys et al. 2006), and may be a universal trait associated with intermediate-to-mature-age Pacific Northwest conifer forests.

Old-growth E_T varied little (Δ=3 mm) between the 2006 and 2007 summer months even though rainfall and average θ_v showed that 2007 was wetter. While it is true that there is some uncertainty involved with E_T measurements, the uncertainty should remain the same from year to year at each site as long as the IRGA is carefully calibrated. We inadvertently introduced different instrument-related errors by using a closed-path IRGA at the old-growth stand and an open-path IRGA at the early seral stands. In lieu of assessing the instrument errors directly, we used bootstrapping to quantify uncertainties on E_T. The results showed that the differences in E_T from the early seral stands and the old-growth forest were significant.

If we add to our chronosequence an initiation stage Douglas-fir stand from Vancouver Island (Humphreys et al. 2006) and two young Douglas-fir stands from Wind River (Chen et al. 2004) then the 0–3 year, 20-year, and 40-year-old age classes are also available for comparison. Figure 6 summarizes the available EC data and shows significant stand-age differences in the mean midday July, August, and September CO_2 fluxes. Highest to lowest rates of net carbon uptake occurred in the 40-year old stand, 20-year old stand, early seral stands (~10 years old), old-growth stand, and initiation stand during July-September. The initiation stand shows the smallest CO_2 fluxes but is still a net CO_2 sink during summer-time midday hours (Humphreys et al. 2006).

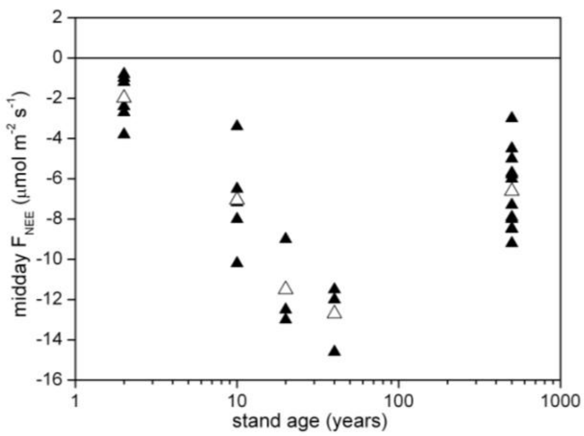

Figure 6. Late-summer CO_2 fluxes for a Pacific Northwest Douglas-fir chronosequence. Plotted are mean midday F_{NEE} during July-September. Sites include the Vancouver initiation stand (2-3 years, measured in 2002 and 2003, Humphreys et al. 2006), Wind River early seral (0-15 years, measured in 2006 and 2007), Wind River 20-year old (measured in 1999, Chen et al. 2004), Wind River 40-year old (measured in 1998, Chen et al. 2004), and Wind River old-growth stand (shown for 1998,1999, 2006, 2007). Open triangles are the stand mean F_{NEE}.

6. CONCLUSION

This study reports crucial data for two rarely studied age classes: early seral and old-growth. Data such as these are necessary for understanding how stand-age affects ecosystem exchange of carbon dioxide, water and energy. Our results show how highly sensitive the early seral age class is to weather anomalies and phenological events. Our study also sheds light on how important it is to quality-control daytime fluxes based on footprint estimates and ABL turbulence statistics in small clear-cuts to ensure that the eddy covariance technique is valid in forest stands with limited fetch. U^* is not the best turbulence parameter for determining daytime stability. U_{TKE} is better suited because it includes both mechanically and thermally produced sources of turbulence, as would be present during daylight hours.

7. ACKNOWLEDGEMENTS

This research was funded by the Western Regional Center (WESTGEC) of the National Institute for Global Environmental Change (NIGEC) through the U.S. Department of Energy (Cooperative Agreement No. DE-FC03-90ER61010) and the Jastro Shields Graduate Research Scholarship (UC Davis). WRCCRF is operated under joint sponsorship of the University of Washington and the USDA Forest Service/PNW Station and we acknowledge both for significant support. Lawrence Livermore National Laboratory is operated by Lawrence Livermore National Security, LLC, for the U.S. Department of Energy, National Nuclear Security Administration under Contract DE-AC52-07NA27344. Any opinions, findings, and conclusions or recommendations expressed herein are those of the authors and do not necessarily reflect the view of DOE. LLNL-PROC-445252

8. REFERENCES

Acevedo, O.C., Moraes, O.L., Degrazia, G.A., Fitzjarrald, D.R., Manzi, A.O., Campos, J.G., 2009: Is friction velocity the most appropriate scale for correcting nocturnal carbon dioxide fluxes? *Agric. For. Meteorol.*, 149, 1–10.

Aubinet, M., Grelle, A., Ibrom, A., et al., 2000: Estimates of the annual net carbon and water exchange of forests: the Euroflux methodology. *Adv. Ecol. Res.*, 30, 113–175.

Chen, J.Q., Paw U, K.T., Ustin, S.L., Suchanek, T.H., Bond, B.J., Brosofske, K.D., Falk, M., 2004: Net ecosystem exchanges of carbon, water, and energy in young and old-growth Douglas-fir forests. *Ecosystems*, 7, 534–544.

Cohen, W.B., Harmon, M.E., Wallin, D.O., Fiorella, M., 1996: Two decades of carbon flux from forests of the Pacific Northwest. *Bioscience*, 46, 836–844.

Falk, M., 2005: Carbon and energy exchange between an old-growth forest and the atmosphere. Ph.D. Dissertation, University of California, Davis, California, pp 196.

Falk, M., Paw U, K.T., Wharton, S., Schroeder, M., 2005: Is soil respiration a major contributor to the carbon budget within a Pacific Northwest old-growth forest? *Agric. For. Meteorol.*, 135, 269–283.

Falk, M., Wharton, S., Schroeder, M., Ustin, S., Paw U, K.T., 2008: Flux partitioning in an old growth forest: seasonal and interannual dynamics. *Tree Physiol.*, 28, 509–520.

Feigenwinter, C.C., Bernhofer, C., Vogt, R., 2004: The influence of advection on the short-term CO2 budget in and above a forest canopy. *Boundary-Layer Meteorol.*, 113, 201–224.

Goulden, M.L., Munger, J.W., Fan, S.-M., Daube, B.C., Wofsy, S.C., 1996: Measurements of carbon sequestration by long-term eddy covariance measurements and a critical evaluation of accuracy. *Global Change Biol.*, 2, 169–182.

Harmon, M.E., Bible, K., Ryan, M.G., Shaw, D.C., Chen, H., Klopatek, J., Li, X., 2004: Production, respiration, and overall carbon balance in an old-growth *Pseudotsuga-Tsuga* forest ecosystem. *Ecosystems*, 7, 498–512.

Humphreys, E.R., Black, T.A., Morgenstern, K., Li, Z., Nesic, Z., 2005: Net ecosystem production of a Douglas-fir stand for 3 years following clearcut harvesting. *Global Change Biol.*, 11, 450–464.

Humphreys, E.R., Black, T.A., Morgenstern, K., Cai T., Drewitt, G.B., Nesic, Z., Trofymow, J.A., 2006: Carbon dioxide fluxes in coastal Douglas-fir stands of different stages of development after clearcut harvesting. *Agric. For. Meteorol.*, 140, 6–22.

Irvine, M.R., Gardiner, B.A., Hill, M.K., 1997: The evolution of turbulence across a forest edge. *Boundary Layer Meteorol.*, 84, 467–486.

Kljun, N., Rotach, M.W., Schmid, H.P., 2002: A 3D backward Lagrangian footprint model for a wide range of boundary layer stratifications. *Boundary-Layer Meteorol.*, 103, 205–226.

Kljun, N., Calanca, P., Rotach, M.W., Schmid, H.P., 2004: A simple parameterization for flux footprint predictions. *Boundary-Layer Meteorol.*, 112, 503–523.

Kolari, P., Pumpanen, J., Rannik, U., Ilvesniemi, H., Hari, P., Berninger, F., 2004: Carbon balance of different aged Scots pine forests in Southern Finland. *Global Change Biol.*, 10, 1106–1119.

Kruijt, B., 1994: Turbulence over forests, downwind of an edge. Ph.D. Dissertation, University of Groningen.

Lee, X.H., 1998: On micrometeorological observations of surface-air exchange over tall vegetation. *Agric. For. Meteorol.*, 91, 39–49.

Marcolla, B., Cescatti, A., Monyagnani, L, Manca, G., Kerschbaumer, G., Minerbi, S., 2005: Importance of advection in the atmospheric exchanges of an alpine forest. *Agric. For. Meteorol.*, 130, 193–206.

Massman, W.J., Lee, X., 2002: Eddy covariance flux corrections and uncertainties in long-term studies of carbon and energy exchanges. *Agric. For. Meteor.*, 113, 121–144.

Papale, D., Reichstein, M., Aubinet, M., et al., 2006: Towards a standardized processing of Net Ecosystem Exchange measured with eddy covariance technique: algorithms and uncertainty estimation. *Biogeosciences*, 3, 571–583.

Park, Y.-S., Paw U, K.T., 2004: Numerical estimations of horizontal advection inside canopies. *J. Applied Meteorol*., 43, 1530–1538.

Parker, G.S., Chen, J., Harmon, M.E., et al., 2004: Three-dimensional structure of the old-growth *Pseudotsuga-tsuga* canopy and its implications for radiation balance, microclimate, and gas exchange. *Ecosystems,* 7, 440–453.

Paw U, K.T., Baldocchi, D., Meyers, T.P., Wilson, K.B., 2000: Correction of eddy-covariance measurements incorporating both advective effects and density fluxes. *Boundary-Layer Meteorol.*, 91, 487–511.

Paw U, K.T., Falk, M., Suchanek, et al., 2004: Carbon dioxide exchange between an old-growth forest and the atmosphere. *Ecosystems*, 7, 513–524.

Reichstein, M., Falge, E., Baldocchi, D., Papale, D., et al. 2005: On the separation of net ecosystem exchange into assimilation and ecosystem respiration: review and improved algorithm. *Global Change Biol.*, 11, 1424–1439.

Schmid, H.P., 1994: Source area for scalars and scalar fluxes. *Boundary-Layer Meteorol.*, 67, 293–318.

Shaw, D.C., Franklin J.F., Bible, K., Klopatek, J., Freeman, E., Greene, S., Parker, G.G., 2004: Ecological setting of the Wind River old-growth forest. *Ecosystems*, 7, 427–439.

Song, C., Woodcock, C.E., 2002: Effects of stand age structure on regional carbon budgets of forest ecosystems. *Eos Trans. AGU, 83*(47), Fall Meet. Suppl., Abstract B12B-0812.

Stull, R.B., 1988: An Introduction to Boundary Layer Meteorology. Kluwer Academic Publishers, The Netherlands, 670 p.

van Breugel, P.B., Klaassen, W., Moors, E.J., 1999: Fetch requirements near a forest edge. *Phys Chem Earth* (B) 24, 125–131.

Webb, E.K., Pearman, G.I., Leuning, R., 1980: Correction of flux measurements for density effects due to heat and water-vapor transfer. *Quart. J. Roy. Meteorol. Soc.,* 106, 85–100.

Wharton, S., Schroeder, M., Paw U, K.T., Falk, M., Bible, K., 2009a: Turbulence considerations for comparing ecosystem exchange over old-growth and clear-cut stands for limited fetch and complex canopy flow conditions. *Agric. For. Meteor.*, 149, 1477-1490.

Wharton, S., Schroeder, M., Bible, K., Falk, M., Paw U, K.T. 2009b: Stand-level gas-exchange responses to seasonal drought in very young versus old Douglas-fir forests of the Pacific Northwest, USA. *Tree Phys.*, 29, 959-974.

Wilson, J., Swaters, G., 1991: The source area influencing a measurement in the PBL: “the footprint”. *Boundary-Layer Meteor.*, 55, 25–46.